

ENABLING THE IMPLEMENTATION OF SPATIAL INTERWEAVE LTE COGNITIVE RADIO

Boris Kouassi, Dirk Slock, Irfan Ghauri, Luc Deneire

kouassi@i3s.unice.fr, slock@eurecom.fr, ghauri@intel.com, deneire@i3s.unice.fr

ABSTRACT

LTE the latest mobile network standard, is widely adopted and targets high spectral efficiency. Cognitive radio (CR) systems on the other hand enable smart use of wireless resources leading to significant performance and reliability improvement. Accordingly, adopting the LTE specifications in CR it is a reasonable choice to optimized the spectrum utilisation in wireless communications. In this paper, we investigate some issues in the real-time implementation of a TDD (time division duplex) LTE-based spatial interweave (IW) CR. Indeed, the IW-CR requires the channel state information (CSI) to opportunistically exploit spatial holes for cognitive transmissions. Preliminary works have illustrated the possibility to acquire the CSI through the calibration of the channel reciprocity inherent in TDD systems. However, they consider constant radio frequency (RF) filters, which leads to perturbations in the IW-CR. Hence, we propose a new tracking method to tackle the variation in the RF. The whole system is implemented and evaluated on an experimental platform, where the simulation results reveal performance enhancement using this new approach.

Index Terms— Cognitive Radio, LTE-TDD, Reciprocity-Calibration, Precoding, Channel Estimation.

1. INTRODUCTION

The LTE (Long Term Evolution) is a recent evolution of cellular standards developed by the 3rd generation partnership project (3GPP) [1]. It targets high spectral efficiency and is widely adopted around the world as near 4G standard. Besides, cognitive radio (CR) which enables smart use of radio resources, is a key ingredient to achieve high spectral efficiency [2]. Consequently, it is a natural choice to exploit the LTE specifications in CR (CR-LTE) in order to enable the wide adoption of cognitive radio and eventually to optimized the spectrum management in wireless systems. In addition, the LTE standard has been designed with a high flexibility which allows the integration of innovative technologies like CR.

B. Kouassi and L. Deneire ({kouassi, deneire}@i3s.unice.fr) are with the laboratory I3S at the University of Nice Sophia Antipolis, France. D.T.M. Slock (slock@eurecom.fr) is with Mobile Communications Department of EURECOM, Sophia Antipolis, France. I. Ghauri (ghauri@intel.com) is with Intel Mobile Communications, Sophia Antipolis, France.

Furthermore, a review of literature indicates that the idea of exploiting the advantages of CR in LTE is not new (see e.g. [3, 4]). Likewise in [5] authors have suggested the implementation of a spatial interweave LTE-TDD (time division duplex) CR scenario on the EURECOM OpenAirInterface (OAI) experimental platform (<http://www.openairinterface.org>). This implementation is based on the key assumption of the channel reciprocity that occurs in TDD systems and aims at mitigating the interferences generated from the secondary system towards the primary. Nonetheless, due to the radio frequency (RF) discrepancies, an initial calibration procedure is mandatory to restore and to exploit the channel reciprocity assumption. This calibration constraint generally related to the most reciprocity-based implementations is a fundamental condition. Accordingly, the reciprocity-calibration allows to override a major problem in the practical implementation of LTE spatial interweave CR.

Preliminary studies have evaluated different reciprocity calibration schemes (see e.g [6, 7]), while others have focused on the calibration implementation in a IW-CR scenario [4, 5]. However, the IW precoding and the reciprocity-calibration was achieved in two different phases. This leads to some interferences from the cognitive users during the channel estimations and the calibration process.

Subsequently, a review of literature shows that the variation of the RF front-ends (RF) is so far not really considered [6, 8], whereas all these drawbacks can eventually decrease the performance of the whole system. Similarly, in early review of literature i.e. [8] authors have mentioned the necessity of frequent calibration cycles, especially when the environment in close proximity of the antennas is potentially changing.

The approach outlined in this study suggests a *tracking* scheme allowing to find constantly the variation of the RF in order to update the calibration factors, and a solution to calibrate the channel when the IW beamformer is activated.

2. SYSTEM MODEL AND BACKGROUNDS

2.1. System Model

The system model is described in the Fig. 1 and follows the conceptual framework of our previous studies [4]. The system is designed with 4 users (2 primary and 2 secondary). The secondary LTE base station denoted eNB2, uses 2 antennas while all the other terminals use 1 antenna. Assuming

only the secondary point to point MISO system in a multipath channel, the received signal at the user side in time domain $y(t)$ is expressed such:

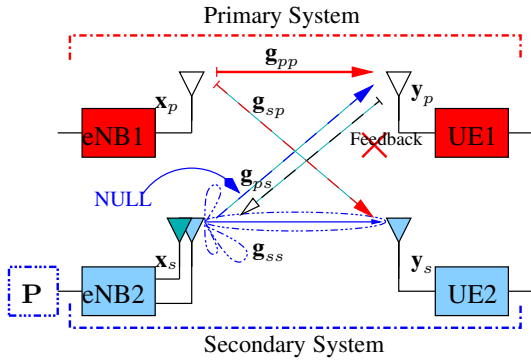


Fig. 1. System model illustrating the downlink transmission with the primary users and the secondary (cognitive) terminals using a precoder to cancel the interference towards the primary user.

$$y(t) = \mathbf{g}_0(t, \tau) * x_0(t) + \mathbf{g}_1(t, \tau) * x_1(t) + n(t), \quad (1)$$

with $(*)$ the convolution symbol, $x(t)$ the transmitted signal in time domain, $n(t)$ the AWGN at the receiver, $\mathbf{g}_i(t, \tau)$ the downlink (DL) channel for the i th antenna, τ represents the delay spread depending on the taps generated by the multipath channel. The OFDM multiplexing adopted on the OAI platform allows to write the frequency selective channel into several parallel simple AWGN channels on sub-carriers in frequency domain, leading to: $\mathbf{y}[\nu] = \mathbf{DFT}\{\mathbf{y}(t)\}$ (discrete Fourier transform). As already illustrated in [5], the interference cancellation approach is a zero forcing precoding implemented in the secondary LTE base station (eNB2). The per-subcarrier received signal ($\mathbf{y}_p \in \mathbb{C}$) at the primary user (UE1) in the DL configuration is expressed by:

$$\mathbf{y}_p = \mathbf{g}_{pp}\mathbf{x}_p + \mathbf{g}_{ps}\mathbf{x}_s + \mathbf{n}, \quad (2)$$

with \mathbf{n} the frequency domain AWGN introduced at the PU receiver side. The interference generated by the secondary transmitter is expressed by the term: $\mathbf{g}_{ps}\mathbf{x}_s$. According to the spatial interweave cognitive radio approach adopted in this paper, the following section will describe how the precoding is applied in the secondary system in order to automatically cancel the secondary interference term.

2.2. Precoding Scheme

We aim at sending a null interference in the direction of UE1, this yields to automatically cancel the term $\mathbf{g}_{ps}\mathbf{x}_s = 0$. A solution is to design a precoder \mathbf{p} at eNB2 such as $\mathbf{x}_s = \mathbf{p}\mathbf{s}_x$, with \mathbf{s}_x the transmitted symbol at eNB2. In order to fulfill

this condition, we propose to design $\mathbf{p} = [p_1 \ p_2]$ such as:

$$\begin{aligned} \mathbf{g}_{ps}\mathbf{x}_s &= [g_{ps1} \ g_{ps2}] \begin{bmatrix} x_{s1} \\ x_{s2} \end{bmatrix} = 0, \\ \mathbf{g}_{ps}\mathbf{p}\mathbf{s}_x &= [g_{ps1} \ g_{ps2}] \begin{bmatrix} p_1 \cdot s_{x1} \\ p_2 \cdot s_{x2} \end{bmatrix} = 0, \end{aligned}$$

The precoder \mathbf{p} uses the crosslink DL channel estimation $\hat{\mathbf{g}}_{ps} = [\hat{g}_{ps1} \ \hat{g}_{ps2}]$ in order to cancel the interference from secondary to primary such as:

$$g_{ps1}p_1 + g_{ps2}p_2 = 0; \quad p_1 = g_{ps2}, p_2 = -g_{ps1}. \quad (3)$$

Due to the lack of cooperation between primary and secondary (see Fig. 1) we propose to acquire this crosslink channel using the channel reciprocity that occurs in TDD systems. Nevertheless, the perturbations introduced by the radio frequency circuits (RF) leads to first calibrate the system in order to restore the channel reciprocity. Hence, the efficiency of the precoder \mathbf{p} will be related to the reliability of the crosslink channel estimated using the reciprocity-calibration.

Although much work about the implementation of calibration in the LTE OAI platform has been done to date (see e.g. [6, 5]), more studies need to be conducted to ascertain the possible impact of the RF filter variations. In addition, it is important to emphasize the fact that the IW precoding process in the previous investigations [5] was separated with the reciprocity-calibration step. This suggests possible interferences from secondary to the primary during the (re)calibration and the channel estimation phases. All these observations can eventually disturb the whole system and reduce the performances. In the following section we describe our proposal to improve the calibration process.

3. RECIPROCITY-CALIBRATION

We note that the TDD RF front-ends are composed by electronic components as illustrated in Fig. 2 [4, 5]. Therefore, their properties (impulse response, etc) vary according to the temperature and close-by elements (human hands, etc) as illustrated in [8]. It is then reasonable to propose some methods allowing to compensate for the RF impacts and variations.

3.1. Initial Calibration Implementation in OAI

The current algorithm of RF relative calibration in the OAI simulator platform is designed based on the 10 ms LTE-TDD frame configuration 3 composed by 10 uplink (UL) and downlink (DL) subframes as illustrated in Fig. 3 [4, 9]. It proposes to collect several versions of the uplink UL and the DL channels over the time, and then to infer the calibration parameters for the 2 antennas of the eNB2 denoted \mathbf{c}_{s_1} and \mathbf{c}_{s_2} . The calibration is achieved in exploiting the information contained in the DL ($\mathbf{g}_{ss} = [g_{s1}, g_{s2}]$) and its corresponding UL channels ($\mathbf{h}_{ss} = [h_{s1}, h_{s2}]$). The parameters \mathbf{c}_{s_1} and \mathbf{c}_{s_2} will be used

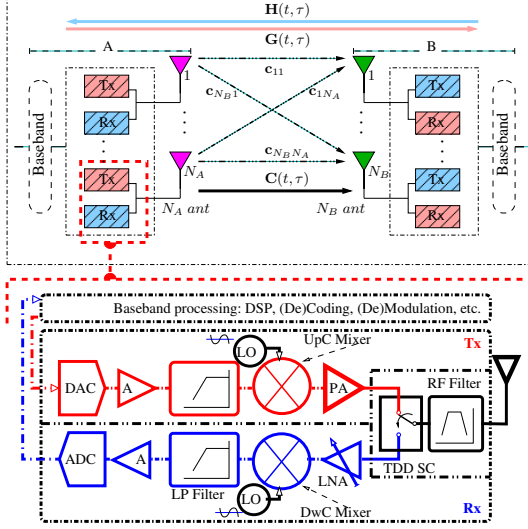


Fig. 2. Example of conventional TDD RF front-ends circuits.

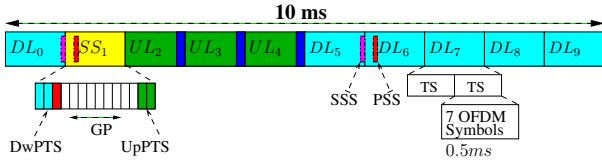


Fig. 3. OAI TDD-LTE frame specifications including the primary and secondary synchronization signals (PSS/SSS), the guard period (GP), and the DL/UL pilot time slot Dw/UpPTS.

to find automatically the DL crosslink channel \mathbf{g}_{ps} without any feedback. Finally, the information provided by the determined crosslink channel \mathbf{g}_{ps} will be exploited to design the zero forcing beamformer.

In the calibration step, the problem is simplified in subdividing the multi-input single-output (MISO) secondary user channel into several single channels and then uses a (total least squares) TLS technique to solve the calibration. More concretely, the algorithm restores the reciprocity assumption by finding the calibration parameters $\mathbf{c}_s = [\mathbf{c}_{s1}, \mathbf{c}_{s2}]$ consisting of RF parameters like $\mathbf{g}_{ss} = \mathbf{c}_s \mathbf{h}_{ss}^T$. In order to improve the estimation of calibration parameters in noisy channel, we consider K versions of the channel across the time assuming that calibration factors vary slowly in time. Let's write $\hat{\mathbf{G}}_{SS}$ and $\hat{\mathbf{H}}_{SS}$ respectively the DL and UL concatenated channel between the two antennas at eNB2 and the antenna at UE2. The equation is finally reformulated into TLS problem such:

$$\begin{aligned} & \min_{\mathbf{c}_s} \left(\|\tilde{\mathbf{H}}_{SS}\|^2 + \|\tilde{\mathbf{G}}_{SS}\|^2 \right) \\ & \text{s.t.} \quad \left(\hat{\mathbf{H}}_{SS} + \tilde{\mathbf{H}}_{SS} \right) \mathbf{c}_s = \left(\hat{\mathbf{G}}_{SS} + \tilde{\mathbf{G}}_{SS} \right), \end{aligned} \quad (4)$$

where $\tilde{\mathbf{H}}_{SS}$ and $\tilde{\mathbf{G}}_{SS}$ are the estimation error correction. \mathbf{c}_s is finally found with the singular value decomposition (SVD) solution of the TLS problem presented in [10].

3.2. New Auto-Calibration Approach

So far, in the implementation on OAI described above, the precoding and the calibration phase were achieved alternatively in 2 different steps [9, 4, 5]. This leads to some major drawbacks like the interference generated during the channel estimations and the calibration phases because the precoding is deactivated. The variations in the RF filters and the frequency offset yields as well incorrect calibration parameters in the precoding. First we assume the precoding not activated during the calibration step, then the per-subcarrier DL channel \mathbf{g}_{ss} is estimated such as:

$$\hat{\mathbf{g}}_{ss} = \mathbf{y}_s \mathbf{s}_s^* = (g_{ss1} \cdot s_{x1} + g_{ss2} \cdot s_{x2} + n_p) \begin{bmatrix} s_{x1}^* & s_{x2}^* \end{bmatrix}, \quad (5)$$

where \mathbf{s}_x is the pilot known at the transmitter and the receiver. In order to keep the pilot orthogonal in LTE, the pilot s_{x1} for antennas 1 and s_{x2} for antenna 2 are located in two different resource elements in the LTE resource block [1]. Thereby, the UE is able to estimate the channel coefficient with the first antenna of the eNB2 in the first resource element such $\hat{g}_{ss1} = \mathbf{y}_s s_{x1}^* (s_{x2} = 0)$, and for the second antenna of eNB2 in the second resource element using $\hat{g}_{ss2} = \mathbf{y}_s s_{x2}^* (s_{x1} = 0)$.

The precoding efficiency at the eNB2 is guaranteed by the accuracy of the DL channel obtained after the reciprocity-calibration. Therefore, the calibration factor should be updated periodically even if as mentioned above, we suppose the RF parameters vary slowly in time. In order to keep a reliable calibration factor in time, we propose a "tracking" calibration process such that in some specific UL subframes, the DL channels from the UE2 to the eNB2 is periodically feedback. Furthermore, to be able to estimate the channel from eNB2 antenna 0 and 1 in the LTE transmission mode 1, we have performed a modification in the initial LTE special subframe (SS, see Fig. 3) [5]. Therefore, using the DL channel estimation in the SS, a new factor is computed for each frame at the eNB2 like illustrated in the following relation:

$$\begin{aligned} \mathbf{c}_1 \begin{bmatrix} \mathbf{h}_{s1} \\ \vdots \\ \mathbf{h}_{sK} \end{bmatrix} &= \begin{bmatrix} \mathbf{g}_{s1} \\ \vdots \\ \mathbf{g}_{sK} \end{bmatrix}, \mathbf{c}_2 \begin{bmatrix} \mathbf{h}_{s(K+1)} \\ \vdots \\ \mathbf{h}_{sK} \end{bmatrix} = \begin{bmatrix} \mathbf{g}_{s(K+1)} \\ \vdots \\ \mathbf{g}_{sK} \end{bmatrix}, \dots \\ \dots, \mathbf{c}_{N-K} \begin{bmatrix} \mathbf{h}_{s(N)} \\ \vdots \\ \mathbf{h}_{s(K+n)} \end{bmatrix} &= \begin{bmatrix} \mathbf{g}_{s(N)} \\ \vdots \\ \mathbf{g}_{s(K+n)} \end{bmatrix}, n < N, \end{aligned} \quad (6)$$

where N represents the number of frames used for the experimentation. This approach allows to achieve the calibration in the precoding step without disrupting the whole process.

However, we note in this formulation that the fast or slow variation of the RF will influence the choice for the value of K . Indeed, K can be kept large for a slow variation, since the overall calibration factors will be highly correlated in the time. Nevertheless, if the RF vary quickly a small value of K will be beneficial.

Furthermore, as mentioned in [7] and simulated in [11, 5], due to the up/down converters, a residual frequency offset in the successive channel estimations can also occur in the calibration process. This residual frequency offset is cumulative and generates some calibration errors. Thus, it yields an incorrect DL channel reconstruction since the relation between the K UL/DL channels for each antenna becomes:

$$\mathbf{c}_s \begin{bmatrix} \mathbf{h}_{s1} \\ \vdots \\ \mathbf{h}_{sK} \end{bmatrix} = \begin{bmatrix} e^{j2\pi f_o t_1} \mathbf{g}_{s1} \\ \vdots \\ e^{j2\pi f_o t_K} \mathbf{g}_{sK} \end{bmatrix}, \quad (7)$$

where f_o denote for the frequency offset between the up and the down converters, and t_k the acquisition time of the k^{th} channel. Due to the small value of the residual frequency offset (Hz order), the use of conventional offset estimators is limited. However, in [11], authors have solved this problem, using a modified TLS formulation. In this paper, the impact of the residual frequency offset on the tracking approach illustrated in relation (6) will be evaluated in the Section 4.

3.3. Calibration on Precoded Channels

Moreover, when the precoding process in the eNB2 is activated, the transmitted DL signal from eNB2 to UE2 is also precoded. Accordingly, the secondary signal \mathbf{y}_s received at the UE2 is expressed as:

$$\mathbf{y}_s = \mathbf{g}_{ss} \mathbf{x}_s + n_p = g_{ss1} \cdot p_1 \cdot s_{x1} + g_{ss2} \cdot p_2 \cdot s_{x2} + n_p, \quad (8)$$

with $n_p = \mathbf{g}_{sp} \mathbf{x}_p + n$. We note that the estimation of the channel coefficient associated with the first antenna of eNB2 yields to the relation $\mathbf{y}_s s_{x1}^* \approx \widehat{g_{ss1}} \cdot p_1$ which is a combination of the precoder and the DL channel coefficient. This prevents the use of the received feedback parameters directly in the previous calibration algorithm. However, since \mathbf{p} is known at the eNB2, it is possible to compensate for the precoder coefficients (e.g., p_1) in the channel calibration. The relation $\mathbf{g}_{ss} = \mathbf{c}_s \mathbf{h}_{ss}^T$, allows to write $g_{ss1} \cdot p_1 = c_{s1} \cdot h_{ss1} \cdot p_1$. Then we exploit the precoding factors known at the eNB2 onto K channel instances (in time) to find the calibration factors in each MIMO link through the relation:

$$\mathbf{c}_s \begin{bmatrix} \mathbf{h}_{s1} \cdot \mathbf{p}_1 \\ \vdots \\ \mathbf{h}_{sK} \cdot \mathbf{p}_K \end{bmatrix} = \begin{bmatrix} \mathbf{g}_{s1} \cdot \mathbf{p}_1 \\ \vdots \\ \mathbf{g}_{sK} \cdot \mathbf{p}_K \end{bmatrix}. \quad (9)$$

Using this approach, we can calibrate the system even when the precoding procedure is activated at the eNB2. In the next section we will investigate the performance of the proposed calibration approaches.

4. NUMERICAL RESULTS

The efficiency of the proposed tracking method is evaluated based on the previous real-time implementation of the spatial interweave in the OAI simulator [5]. The new calibration

approach is integrated in the OAI software part which implements most of the LTE-TDD layers 1 and 2 (PHY / MAC) specifications. We assume the LTE-TDD frame configuration number 3 described in the Fig. 3, where $N \geq 100$ frames are considered for the experimentation. Each antenna at the eNB2 is calibrated individually and for each frame, the DL channel is reconstructed (\mathbf{g}_{rec}) using the calibration factors and the UL channel estimated at the eNB2. We suppose a perfect feedback, and the mean squares error (MSE) of the DL channel reconstructed through the reciprocity-calibration is used for the performance comparison as illustrated in following relation: $MSE = \frac{\|\widehat{\mathbf{g}} - \mathbf{g}_{rec}\|^2}{\|\widehat{\mathbf{g}}\|^2}$. Subsequently, we introduced a simulated variation on the RF filters and a residual frequency offset from 1Hz to 3Hz. The findings illustrated in Fig. 4 and Fig. 5 indicate that when the RF filters are kept constant during the considered experimentation time, the conventional calibration algorithm (*Normal Cal*) calibrates properly the RF perturbations. Nonetheless, when the RF filters vary in time (see *Normal Cal* on Fig. 5) the reconstruction performance collapses. Whereas the tracking method successfully performs the reconstruction and outperforms the normal calibration in presence of variations in the RF filters.

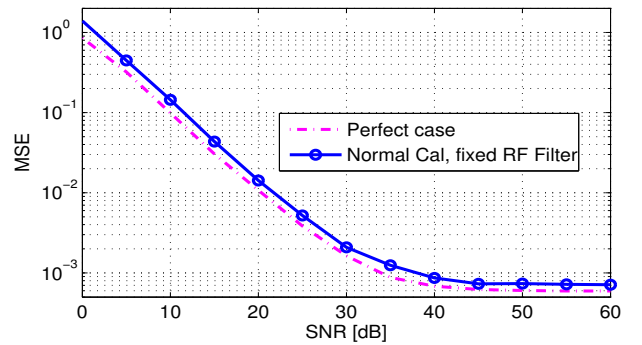


Fig. 4. MSE comparison of the DL channel reconstruction according to the SNR for the eNB2 first antenna with constant RF filters.

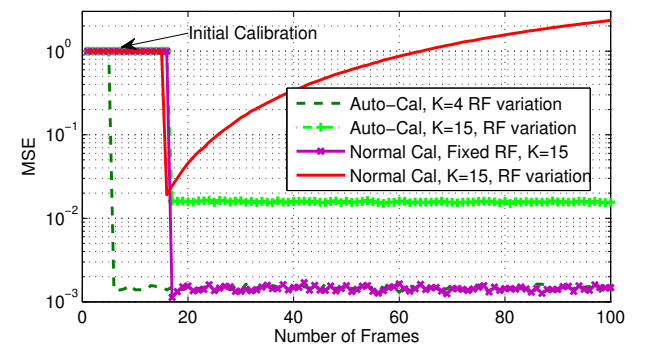


Fig. 5. MSE of the DL channel reconstructions vs the number of frames for the eNB2 first antenna. A residual frequency offset equal to 1Hz is considered for each frame in the RF filters (SNR=30dB).

Furthermore, like mentioned in Section 3.2 and observed

in the Fig. 6, if the number of frames required to calibrate the system (K) increases, the performance of the tracking method decreases. Indeed, in this case, the relation between the calibration factors and the overall UL/DL channels does not correspond to the formulation in the equation (6). Unlike in [9, 5] where it is suggested to overparameterize the calibration TLS equation with a large values of $K \approx [15, 20]$, in the tracking calibration it is beneficial to use a small K in order to reduce the reconstruction errors.

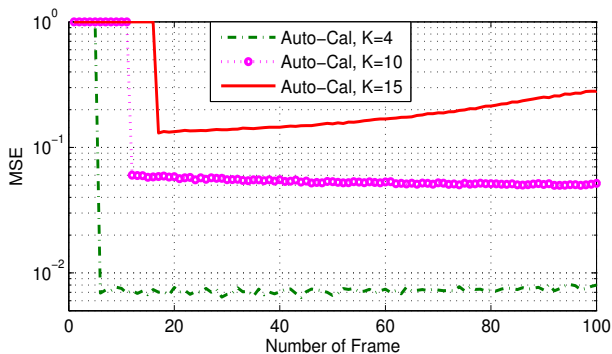


Fig. 6. MSE comparison of the DL channel reconstructions vs the number of frames for the eNB2 first antenna. The cumulative residual frequency offset is increased to 3Hz and the SNR=30dB.

Finally, in Fig. 7 we consider the UL/DL channels Gaussian with i.i.d entries, then we evaluate, the reconstruction capacity when the feedback parameter in the calibration algorithm is a cascade of the DL estimated channel and the precoder. We observe that the proposed calibration technique in Section 3.3 performs the calibration when the precoding is activated and is able to reconstruct the DL channel with approximately the same performance as the case without precoding. The main advantage is to keep reliable calibration

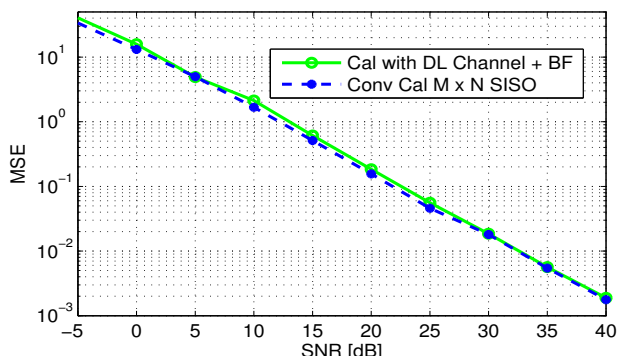


Fig. 7. DL channel reconstructions vs the SNR for one MISO link, when the precoder is activated in a perfect feedback case.

parameters for the beamforming without stopping the precoding process and thereby generating interferences towards the primary UE1.

This study has taken a step in the direction of improving the reciprocity-calibration scheme in TDD-LTE systems.

However, for further implementations, it would be beneficial to extend the study taking into account the reduced payload in the UL, the trade-off between the feedback cycle as well as the complexity.

5. CONCLUSIONS

In this work, we have investigated a practical implementation of TDD-LTE spatial interweave CR implementation. A new TLS-based reciprocity-calibration approach is outlined and evaluated through the CR-LTE simulator in the EURECOM's OpenAirInterface experimental platform. The preliminary simulation results indicate that it is feasible to compensate for the radio frequency filter (RF) impairments even assuming some RF variations in the time. However, further studies needs to be conducted to strengthen the findings and to evaluate the computational complexity as well as the practical considerations in the implementation of this new approach. This will be the subject of future works.

6. REFERENCES

- [1] "3gpp-lte technical specifications," <http://www.3gpp.org/LTE>.
- [2] S. Haykin, "Cognitive radio: brain-empowered wireless communications," *IEEE JSAC*, vol. 23, no. 2, pp. 201–220, 2005.
- [3] Vicente Osa, Carlos Herranz, Jose F Monserrat, and Xavier Gelabert, "Implementing opportunistic spectrum access in lte-advanced," *EURASIP Journal on Wireless Communications and Networking*, vol. 2012, no. 1, pp. 99, 2012.
- [4] B. Zayen, B. Kouassi, R. Knopp, F. Kaltenberger, D. Slock, I. Ghauri, and L. Deneire, "Software implementation of spatial interweave cognitive radio communication using OpenAirInterface platform," in *The Int. Symp. ISWCS*, France, 2012.
- [5] B. Kouassi, B. Zayen, R. Knopp, F. Kaltenberger, D. Slock, I. Ghauri, F. Negro, and L. Deneire, "Design and implementation of spatial interweave lte-tdd cognitive radio communication on an experimental platform," *IEEE Wireless Communications Magazine*, vol. 20, no. 2, pp. 60–67, 2013.
- [6] B. Kouassi, I. Ghauri, B. Zayen, and L. Deneire, "On the performance of calibration techniques for cognitive radio systems," in *The 14th International Symp. WPMC*, France, 2011.
- [7] F. Kaltenberger, H. Jiang, M. Guillaud, and R. Knopp, "Relative channel reciprocity calibration in MIMO/TDD systems," in *IEEE Future Network and Mobile Summit, 2010*, pp. 1–10.
- [8] M. Guillaud, D.T.M. Slock, and R. Knopp, "A practical method for wireless channel reciprocity exploitation through relative calibration," *8th ISSPA, Australia*, pp. 403–406, 2005.
- [9] B. Kouassi, B. Zayen I. Ghauri, and L. Deneire, "Reciprocity calibration techniques, implementation on the OpenAirInterface platform," in *4th Int. Conf. on COGART*, Spain, 2011.
- [10] I. Markovsky and S. Van Huffel, "Overview of total least-squares methods," *Sig. proc.*, vol. 87-10, pp. 2283–2302, 2007.
- [11] M. Guillaud and F. Kaltenberger, "Towards practical channel reciprocity exploitation: Relative calibration in the presence of frequency offset," in *IEEE WCNC Conf. on*, China, 2013.